A Magnetically Geared Lead Screw without Translator Skewing

M. Bahrami Kouhshahi, J. Z. Bird, A. Jannsen
Laboratory for Electromechanical Energy Conversion and Control
Portland State University
Portland, OR, USA
jonathan.bird@ieee.org

J. Kadel, W. Williams
University of North Carolina at Charlotte
Charlotte, NC, USA
wbwillia@uncc.edu

***Abstract*— A magnetically geared lead screw is able to convert high-speed rotation to low-speed translation via magnetic gearing. In this paper a new type of magnetically geared lead screw is presented that uses translator rings without any skewing. The magnetic gearing is accomplished by utilizing an inner rotor with helically skewed magnets and an outer cylinder with a skewed flux focusing magnet arrangement. The operating characteristics and an experimental prototype are presented.**

Keywords*— magnetic gearbox; lead screw; linear actuator; finite element analysis

I. Introduction

Hydraulic actuators are commonly used as linear actuators due to their very high force density and high stiffness [1]. However, hydraulic actuators are typically only efficient over a narrow operating region. In addition, pumps and tubing make their installation complex. Furthermore, the use of hydraulic fluid poses a serious leakage hazard, especially in environmentally sensitive marine environments. As an alternative, electromechanical actuators, are often considered. Electromechanical actuators are typically composed of a mechanical lead screw driven by an electrical motor they can operate with a relatively high force and speed with high accuracy [1]. In comparison to hydraulic actuators, electromechanical actuators are simple to install and are environmentally benign. However, due to the mechanical contact between parts, electromechanical actuators suffer from reliability issues and therefore their operational design life is limited, particularly if regular servicing is not undertaken.

Electromagnetic linear actuators (ELA) create linear motion entirely from the magnetic forces created by a stator and linear translator. An ELA is able to operate at a higher overall efficiency when compared to the hydraulic and electromechanical actuators and non-contact force production results in the reliability being higher than alternative hydraulic and electromechanical actuators. However, the force density of an ELA is constrained by the current density (heat) and magnetic saturation. ELAs have been reported to have volumetric force densities in the range of 0.3 kN/L with air-gap magnetic shear stress values in the range of 83 kN/m^2 [2], [3].

Recently new types of linear actuators, which rely only on magnetic loading, have been proposed to overcome the limitations of the ELAs. Linear magnetic gears (LMG), and magnetic lead screws (MLS) utilizes magnetic field modulation to create linear motion speed change without any physical contact. As the LMG and MLS do not rely on current excitation they have the potential to operate with a significantly higher magnetic shear stress in comparison to the other electromagnetic linear actuators [4]–[16].

The MLS structure is depicted in Fig. 1. It converts linear motion to rotary motion [10]–[16]. Both the magnetic screw and nut in the MLS structure are made of helically shaped radially magnetized permanent magnets. One turn rotation of the inner rotor, makes the translator move by twice the magnet pole-pitch, which is the definition of the inner rotor lead, λ_i. The relationship between angular speed, ω_i, and translating speed, v_i is [11]

$$\omega_i = k_i v_i \tag{1}$$

where the k_i is the wave number and is defined as

$$k_i = 2\pi/\lambda_i \tag{2}$$

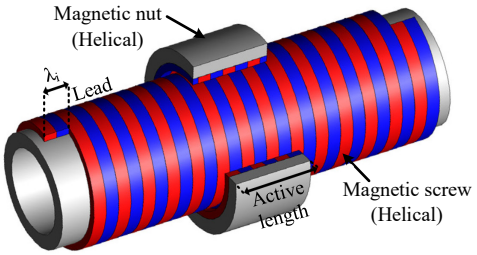

Fig. 1. An example of a magnetic lead screw

The LMG is illustrated in Fig. 2 [4]–[9]. The LMG contains an inner translator with p_i pole-pairs and outer translator with p_o pole-pairs and a central translator with n_t ferromagnetic rings. By selecting the central ferromagnetic rings to equal

$$n_t = p_o + p_i \tag{3}$$

the translators become coupled and if the outer translator is held stationary then the speed relationship between the inner translator and ferromagnetic ring translator is governed by

$$v_i = G_r v_t \tag{4}$$

where the gear ratio is $G_r = n_t/p_i$. The pole-pair and translator lead length for each translator section is shown in Fig. 2. Due to the discrete active length, L, of the LMG the translator lead lengths must be designed to satisfy [17]

$$k_t = k_o \frac{n_t}{p_o} \tag{5}$$

$$k_t = k_i G_r \tag{6}$$

where

$$k_t = 2\pi/\lambda_t \tag{7}$$

$$k_o = 2\pi/\lambda_o \tag{8}$$

If (5) and (6) are not carefully adhered to then the force will be greatly diminished [6].

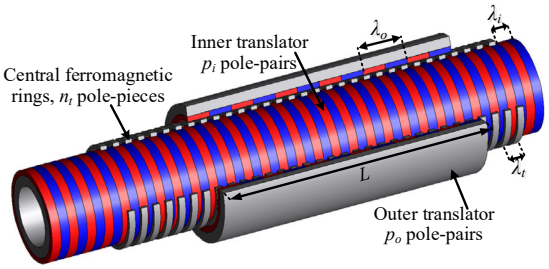

Fig. 2. An example of a linear magnetic gear with p_i=15, p_o= 6, and n_t = 21.

Both the LMG and MLS requires that the translator contain a large quantity of magnet material. This therefore make both the MLS and LMG costly if a large stroke length is required. A new type of magnetically geared lead screw (MGLS), as shown in Fig. 3 was recently proposed in [17] that combines the operating principals of the LMG and MLS. However, unlike the LMG and MLS the translator can be fabricated from only rings of ferromagnetic steel. If the outer cylinder is held stationary, then it was shown in [17] that if the MGLS satisfies (3) as well as (5) and (6) then the translator speed, v_t, will be related to the inner rotor rotational speed, ω_i, by:

$$\omega_i = k_t v_t \tag{9}$$

As the translator and inner rotor wave number are related by (6) the MGLS changes the translational motion into rotational motion via a gearing ratio. The translator force, F_t, and inner rotor torque, T_i, are related by

$$T_i \omega_i - F_t v_t = P_L \tag{10}$$

where P_L is the mechanical and electrical losses. Substituting (9) into (10) and assuming the power loss is relatively small one obtains

$$T_i k_t = F_t \tag{11}$$

Unlike the MLS and LMG the translator stroke length can be made very long without requiring more magnet material. In order for the rotor and translator fields to couple, the MGLS design shown in [17] required that the inner rotor magnets be helically skewed and the translator ferromagnetic rings be axially skewed. Fig. 4 more clearly shows the skewing of the ferromagnetic translator rings. The skewing of the translator rings significantly increases the manufacturing cost of the MGLS as it is difficult to fabricate the skewed rings to a high tolerance. Small tolerance inaccuracies in the rings can also cause the force to reduce significantly when compared to the predicted values [17].

The purpose of this paper is to present a new type of MGLS that does not require the use of skewed translator rings and therefore the design significantly reduces the cost of the MGLS construction.

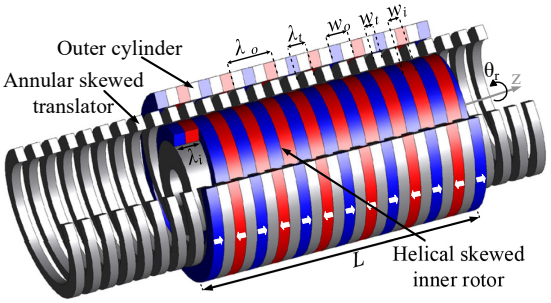

Fig. 3. Structure of the MGLS proposed in [17].

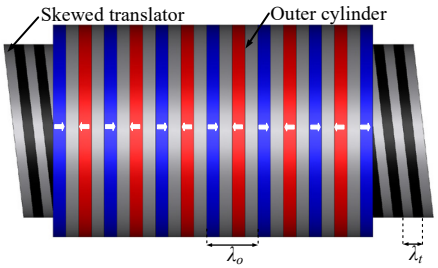

Fig. 4. Side view of the MGLS with skewed translator

II. Magnetically Geared Lead Screw without Translator Skewing

The new MGLS is realized by skewing the outer cylinder poles instead of the translator rings. The geometric and material parameters used in this design analysis are given in Table I. The design has a translator wave number of k_t = 837.75 rad/m. Consider the schematic shown in Fig. 5, the outer cylinder can be skewed by axially shifting a half-ring (180 degrees) of the magnet and ferromagnetic steel by distance L_{sa}. The computed force as a function of axial shift, L_{sa}, is shown in Fig. 6. It can be seen that the peak translator force F_t = 1.462 kN occurs at L_{sa} = 9mm. However, if the half ring outer rotor is shifted by L_{sa} =10mm then this will equal the outer cylinder pole-pitch ($2w_o$). In this case the peak translator force reduces but only by

2%. Therefore, by choosing the half ring shift to be $L_{sa} = 2w_o$ a particularly simple design is achieved since the outer rotor can then be made of complete ferromagnetic rings with half-ring magnets, such a design is illustrated in Fig. 7.

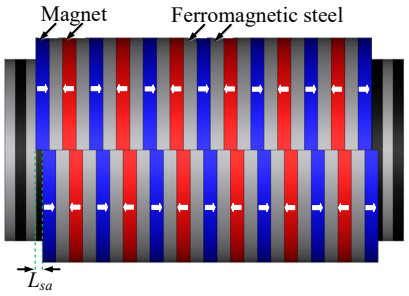

Fig. 5. Parametric design to investigate the effect of the axial shift, L_{sa}, between the top and bottom set of half rings

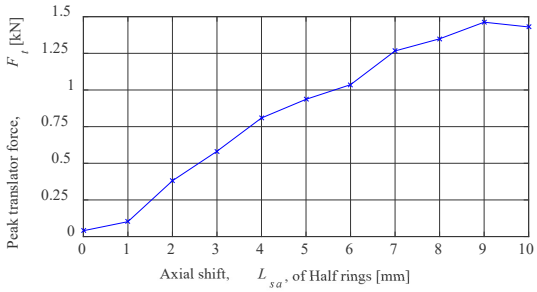

Fig. 6. Maximum translator force versus axial shift, L_{sa} of the half rings

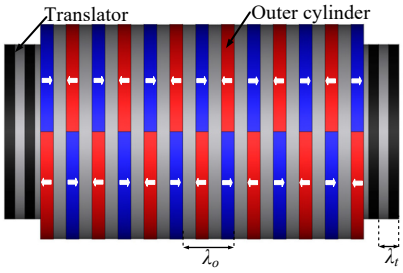

Fig. 7. Proposed new MGLS

TABLE I
GEOMETRIC AND MATERIAL PARAMETERS

Parameter		Value	Unit
Outer cylinder (fixed)	Pole-pairs, p_o	6	-
	Outer radius, r_{oo}	40	mm
	Outer lead length, λ_o	10	mm
	Airgap length, l_g	0.5	mm
	Active axial length, L	120	mm
Translator	Ferromagnetic pieces, n_t	16	-
	Outer radius, r_{to}	32.5	mm
	Radial thickness, l_t	6	mm
	Translator lead length, λ_t	7.5	mm
	Pole-pitch, w_t	3.75	mm
Inner rotor - helically skewed	Pole pairs, p_i	10	-
	Outer radius, r_{io}	26	mm
	Pole-pitch, w_i	6	mm
	Lead, λ_i	12	mm
Material	NdFeB magnet, B_r, NMX-40CH	1.25	T
	1018 steel resistivity	15.9	μΩ-cm

III. OPERATING CHARACTERISTICS

The MGLS demonstrated in previous part (with L_{sa} = 10 mm) was simulated using JMAG FEA software. The radial magnetic flux density due to the inner rotor magnets in the outer airgap with and without translator effect is shown in Fig. 8 and spatial harmonics created by the translator are depicted in Fig. 9. It can be noted that the modulation effect of the translator rings results in a large 6th harmonic being created in the outer air-gap. The same plots for the radial magnetic flux density in the inner airgap when magnets are only present on the outer cylinder are shown in Fig. 10 and Fig. 11.

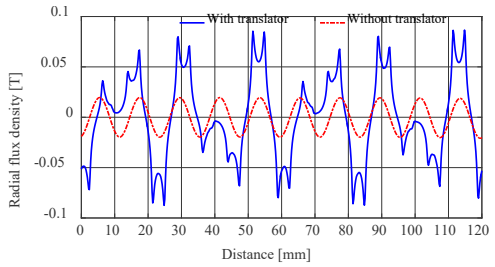

Fig. 8. Radial flux density in the outer airgap (r=32.75mm) when only inner rotor magnets present.

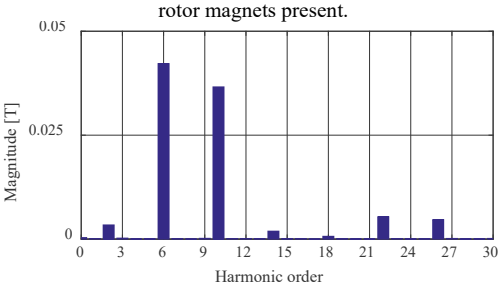

Fig. 9. Harmonic contents of the modulated radial flux density in the outer airgap (r=32.75mm) when only inner rotor magnets present

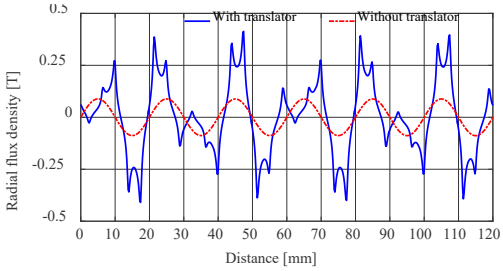

Fig. 10. Radial flux density in the inner airgap (r=26.25mm) when only outer cylinder magnets present.

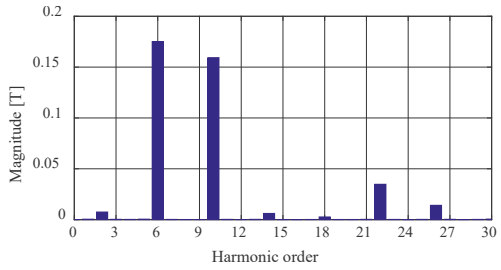

Fig. 11. Harmonic contents of the modulated radial flux density in the inner airgap (r=26.25mm) when only outer cylinder magnets present.

The force and torque on the different parts when the inner rotor is rotated by 360° while the other two parts are stationary, is calculated using a 3-D transient model and the results are shown in Fig. 12 and Fig. 13 respectively. The peak pole slipping force and torque occurs at F_t=1.430 kN and T_t= 1.707 Nm respectively giving a force-to-torque ratio of k_t=837.7 which agrees with (11) when the loss is zero. The values given in Table I (with $L_{sa} = 2w_o$) were used in the analysis. The calculated magnetic shear stress in the inner and outer airgap for this design is 45 kN/m^2 and 23 kN/m^2 respectively.

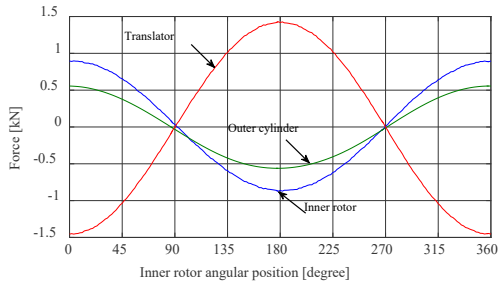

Fig. 12. Force on each MGLS part as a function of inner rotor phase angle

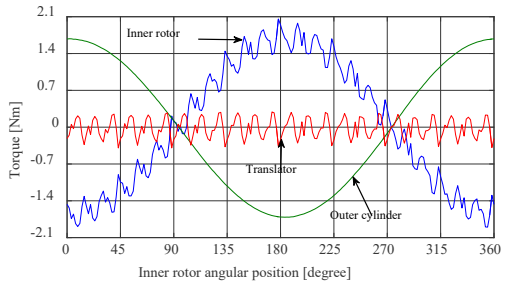

Fig. 13. Torque on each MGLS part as a function of inner rotor phase angle

IV. Experimental Verification

In order to make a comparison with a prior-art design the experimental prototype is based on that presented in [17]. The ideal helical structure for the inner rotor is not practical, therefore a segmented helix structure was used, as shown in Fig. 14. In this structure 60 degree magnet arcs were used. Each helix is formed by 6 segments displaced axially with respect to the adjacent segment. The amount of axial shift, L_{sh}, as defined in Fig. 14, depends on the axial thickness of each segment, w_i, as well as the number of segments in one helix turn, n, therefore:

$$L_{sh} = w_i / (n/2) = 6/(6/2) = 2 \text{ mm} \qquad (12)$$

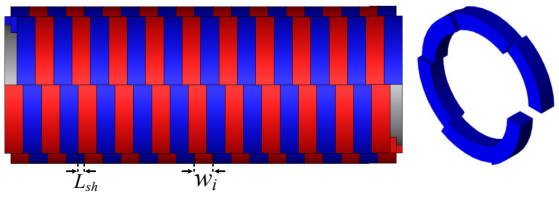

Fig. 14. Side view of the segmented helical inner rotor, and one helix turn

Two sets of rods have been used within the translator rings a cross-sectional view of a translator ring is shown in Fig. 15. The purple sliding rods on the outer and inner radii are used to maintain the airgap and the blue holding rods are used to retain all the rings together. Although, these rods are non-magnetic, the field interaction with the corresponding holes will create field and torque distortions.

Due to past experimental prototype design decisions the axial thickness of the outer cylinder's PMs and steel rings were changed in order to fit all the active material within the active length (L = 120mm). This resulted in the outer lead length being λ_o = 19.2 mm instead of λ_o = 20mm. This design change reduced the calculated peak force to F_t = 1.130 kN. Using a JMAG 3-D FEA simulation the magnetostatic force and torque on the different parts of the MGLS were calculated and the simulation results are shown in Fig. 16 and Fig. 17 respectively. As it could be predicted the practical consideration reduced the output force and torque and changed their shape significantly. A summary of the calculated force and torque values for this and the prior design shown in [17] is given in Table II.

TABLE II
FORCE AND TORQUE COMPARISON

Design		Peak Force [kN]	Peak Torque [Nm]	Airgap shear stress [kN/m^2]	
				Inner	Outer
MGLS with translator skew [17]		1.06	1.265	33	16
MGLS without translator skew	Ideal	1.43	1.707	45	23
	Practical	1.13	1.343	38	18

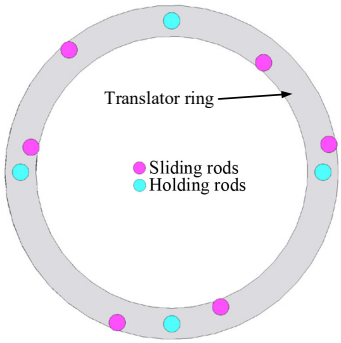

Fig. 15. Cross view of the translator with rods

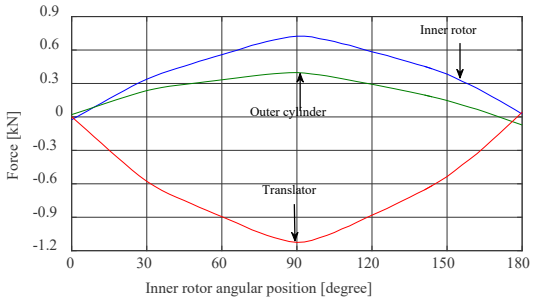

Fig. 16. Calculated force on each MGLS part as a function of inner rotor phase angle

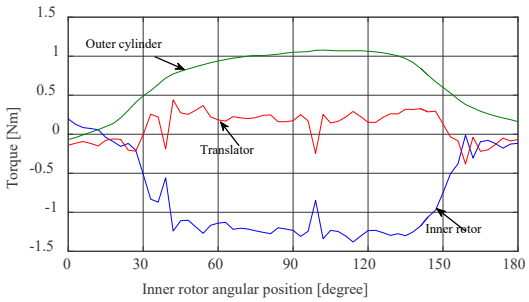

Fig. 17. Torque on each MGLS part as a function of inner rotor phase angle.

Fig. 18 shows the MGLS components. The calculated and measured radial flux density for the inner rotor and outer cylinder are shown in Fig. 19 and Fig. 20 and their corresponding main harmonic orders are compared in Fig. 21 and Fig. 22. As can be seen, the 10th harmonic of the inner rotor flux density is just 0.6% lower than the 10th harmonic of the calculated flux density. This discrepancy is 8.2% for the 6th harmonic of the outer cylinder's flux density. Fig. 23 shows the test setup for the force measurement. The force and torque are currently being measured at the time of this paper submission.

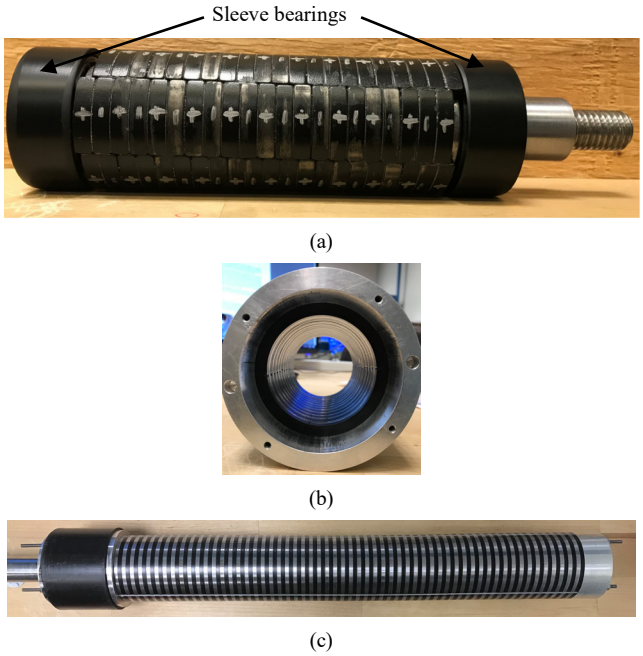

Fig. 18. MGLS components; a) Inner rotor, b) outer cylinder, and c) translator

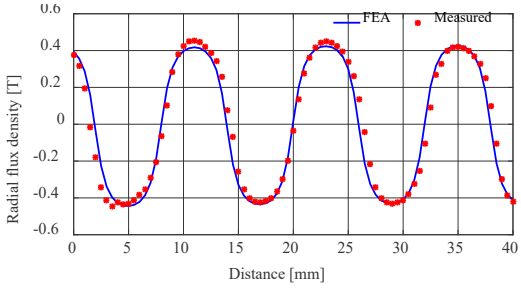

Fig. 19. Calculated and measured flux density at 0.85mm above the surface of inner rotor.

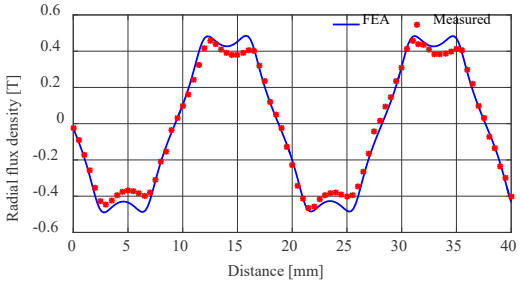

Fig. 20. Calculated and measured flux density and the corresponding main harmonics at 0.85mm above the surface of outer cylinder when they are surrounded by air.

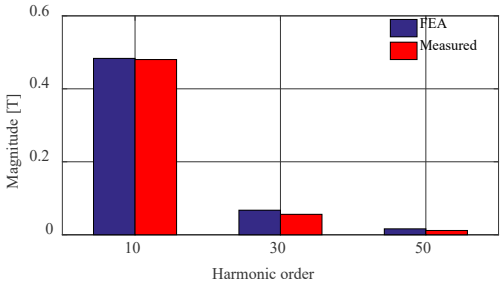

Fig. 21. Main harmonics of the calculated and measured flux density at 0.85mm above the surface of the inner rotor

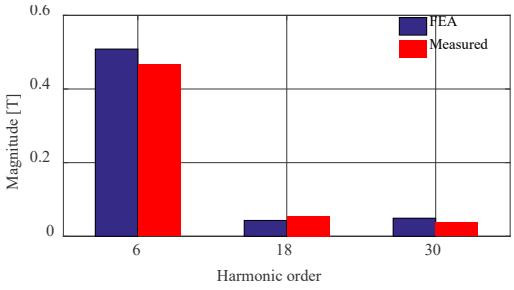

Fig. 22. Main harmonics of the calculated and measured flux density at 0.85mm above the surface of the outer cylinder.

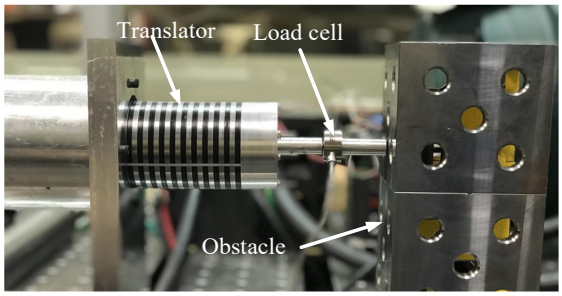

Fig. 23. Test setup for force measurement

V. Conclusion

A new type of MGLS along with an experimental prototype was presented in this paper. The MGLS is unique in that the ferromagnetic rings do not need to be skewed. This therefore results in a significantly simpler and cheaper translator structure. As the translator is made of ferromagnetic steel, the cost of the MGLS in long stroke length applications should be lower than for a LMG and MLS.

ACKNOWLEDGMENT

The authors would gratefully like to thank the JMAG Corporation for the use of their FEA software. This material is based upon work supported by the National Science Foundation under Grant No. 1408310 as well as the North Carolina Coastal Studies Institute.

REFERENCES

[1] J. Xia and W. K. Durfee, "Analysis of Small-Scale Hydraulic Actuation Systems," *J. Mech. Des.*, vol. 135, no. 9, pp. 091001–091001, Jul. 2013.

[2] Y. Fujimoto, T. Kominami, and H. Hamada, "Development and Analysis of a High Thrust Force Direct-Drive Linear Actuator," *IEEE Trans. Ind. Electron.*, vol. 56, no. 5, pp. 1383–1392, May 2009.

[3] N. Bianchi, S. Bolognani, D. D. Corte, and F. Tonel, "Tubular linear permanent magnet motors: an overall comparison," *IEEE Trans. Ind. Appl.*, vol. 39, no. 2, pp. 466–475, Apr. 2003.

[4] K. Atallah, J. Wang, and D. Howe, "A high-performance linear magnetic gear," *J. Appl. Phys.*, vol. 97, no. 10, 2005.

[5] K. Atallah, J. Wang, S. Mezani, and D. Howe, "A Novel High-Performance Linear Magnetic Gear," *IEEJ Trans. Ind. Appl.*, vol. 126, no. 10, pp. 1352–1356, 2006.

[6] R. C. Holehouse, K. Atallah, and J. Wang, "Design and Realization of a Linear Magnetic Gear," *IEEE Trans. Magn.*, vol. 47, no. 10, pp. 4171–4174, Oct. 2011.

[7] W. Li, K. T. Chau, and J. Z. Jiang, "Application of Linear Magnetic Gears for Pseudo-Direct-Drive Oceanic Wave Energy Harvesting," *IEEE Trans. Magn.*, vol. 47, no. 10, pp. 2624–2627, Oct. 2011.

[8] W. Li, Shuang Gao, Diyun Wu, and X. Zhang, "Design of a linear magnetic-geared free-piston generator for series hybrid electric vehicles," in *2010 IEEE Vehicle Power and Propulsion Conference*, 2010, pp. 1–6.

[9] S. Niu, S. L. Ho, and W. N. Fu, "Performance Analysis of a Novel Magnetic-Geared Tubular Linear Permanent Magnet Machine," *IEEE Trans. Magn.*, vol. 47, no. 10, pp. 3598–3601, Oct. 2011.

[10] N. G. Vitale, "Rotary torque-to-axial force energy conversion apparatus," US6190409B1, 1996.

[11] K. Lu and W. Wu, "Electromagnetic Lead Screw for Potential Wave Energy Application," *IEEE Trans. Magn.*, vol. 50, no. 11, pp. 1–4, Nov. 2014.

[12] R. K. Holm, N. I. Berg, M. Walkusch, P. O. Rasmussen, and R. H. Hansen, "Design of a Magnetic Lead Screw for Wave Energy Conversion," *IEEE Trans. Ind. Appl.*, vol. 49, no. 6, pp. 2699–2708, Dec. 2013.

[13] J. Ji, Z. Ling, J. Wang, W. Zhao, G. Liu, and T. Zeng, "Design and Analysis of a Halbach Magnetized Magnetic Screw for Artificial Heart," *IEEE Trans. Magn.*, vol. 51, no. 11, pp. 1–4, Nov. 2015.

[14] N. I. Berg, R. K. Holm, and P. O. Rasmussen, "Theoretical and Experimental Loss and Efficiency Studies of a Magnetic Lead Screw," *IEEE Trans. Ind. Appl.*, vol. 51, no. 2, pp. 1438–1445, Apr. 2015.

[15] S. Pakdelian, N. W. Frank, and H. A. Toliyat, "Magnetic Design Aspects of the Trans-Rotary Magnetic Gear," *IEEE Trans. Energy Convers.*, vol. 30, no. 1, pp. 41–50, Mar. 2015.

[16] J. Wang, K. Atallah, and W. Wang, "Analysis of a Magnetic Screw for High Force Density Linear Electromagnetic Actuators," *IEEE Trans. Magn.*, vol. 47, no. 10, pp. 4477–4480, Oct. 2011.

[17] M. Bahrami Kouhshahi, J. Bird, J. Kadel, and W. Williams, "Designing and experimentally testing a magnetically geared lead screw," *IEEE Trans. Ind. Appl.*, (accepted for publication).